J. Int. Sci. Technol. 2018, 6(1), 1-5 Article

Journal of Integrated
SCIENCE & TECHNOLOGY

Synthesis and characterization of Dendrimer modified Magnetite nanoparticles and their Antimicrobial activity for Toxicity analysis

Neha Sardana[1], Kailash Singh[1], Mukesh Saharan[2], Deepak Bhatnagar[3], Rishabh Shrivastava Ronin[4*]

[1]Centre for Converging Technologies, University of Rajasthan, Jaipur-302004. [2]Department of Physics, School of Basic Sciences. Manipal University, Jaipur - 303007. [3]Department of Physics, University of Rajasthan, Jaipur-302004. [4]Department of Advance Molecular Microbiology (DAMM), Seminal Applied Sciences Pvt. Ltd. Jaipur. Rajasthan - 302015.

Received on: 12-Aug-2017, Accepted and Published on: 05-Jan-2018

ABSTRACT

Interest has been shown in iron magnetite nanoparticles because of its various important properties such as large surface area with high surface-to-volume ratio, ease of separation, water solubility, super paramagnetism and biocompatibility. In addition to this, due to large surface area, dendrimers can also be attached easily. In the present study, Fe_3O_4 magnetic nanoparticles were synthesizedbyco-precipitationmethod and cascading polyamidoaminedendrimersweresynthesized on the surface of these nanoparticles.Structural analysis of these particles was done by XRD and FTIR. SEM showed clear dispersion of the Dendrimer-modified magnetic nanoparticles. Furthermore, antimicrobial activity of these nanoparticles was studied against microbial strains *Escherichia coli* and *Staphylococcus aureus*.

Keywords: Polyamidoamine (PAMAM) Dendrimer, Magnetite Nanoparticle, Antimicrobial Activity.

INTRODUCTION

Metal oxides play a very important role in different areas of physics, materials science and chemistry. They form a large diversity of compounds and can adopt a vast number of structural geometries with an electronic structure that can exhibit metallic, semiconductor or insulator character. They are also used in the fabrication of sensors, piezoelectric devices and microelectronic circuits, fuel cells, anti corrosion coatings and as catalysts.

Magnetic nanoparticles (MNP) have been successfully used in different scientific fields due to their magnetic, biocompatibility and surface modification properties. For example, by using magnetic field, drugs attached to magnetic particle can be delivered to the desired target sites in the body.[1]

Iron oxide nanoparticles have a diameter between 1 - 100 nanometers and are found in two forms; magnetite (Fe_3O_4) and maghemite (γ-Fe_2O_3) which is in its oxidized form. Due to their super paramagnetic properties, they have many potential applications in different fields and are considered better than Co and Ni nanoparticles as these particles are toxic and can be easily oxidized. Surface modified nanoparticles have inner iron oxide core with an outer metallic shell of inorganic materials. The iron oxide nanoparticles have been coated with gold, silica, gadolinium and other suitable elements. This coating provides not only stability to nanoparticles in solution but also helps in binding at nanoparticle surface for various biomedical applications.[2–7] The magnetic nanomaterials also find application in many new smart materials designs and development.[8,9]

Many detailed *in vitro* and *in vivo* studies have shown that magnetic nanoparticles have less toxicity in humans and thus they are being considered as a good candidate for use in drug delivery systems.[1,10–14] For the synthesis of magnetite magnetic nanoparticles co-precipitation method is amongst the most efficient method which can be of further two types. One way is by oxidizing iron (II) hydroxide suspensions by different types of

---

Corresponding Author: Rishabh Shrivastava Ronin
Department of Advance Molecular Microbiology (DAMM), Seminal Applied Sciences Pvt. Ltd. Jaipur. Rajasthan - 302015.
Tel: 8963873909
Email: 134500@gmail.com

Cite as: *J. Int. Sci. Technol., 2018, 6(1), 1-5.*

 ISSN: 2321-4635 http://pubs.iscience.in/jist

oxidizing agents. Using this method, magnetic particles in the range of 30 and 100 nm can be acquired.[13–15]

The second method consists of stoichiometric mixtures of iron (II) and iron (III) hydroxides in aqueous media, yielding consistent round size magnetite particles.[18] In this method, the chemical reaction occurs as follows

$$2Fe^{3+} + Fe^{2+} + 8OH^- \rightarrow Fe_3O_4 + 4H_2O$$

For this reaction optimum conditions are non-oxidizing environment, pH between 8-14 and ratio of Fe^{3+}/Fe^{2+} of (2:1). As it is highly susceptible to oxidation, magnetite (Fe_3O_4) is transformed to maghemite (γFe_2O_3) in the presence of oxygen[19]:

$$2Fe_3O_4 + O_2 \rightarrow 2\ \gamma Fe_2O_3$$

The size and shape of the nanoparticles can be controlled by adjusting pH, temperature, ionic strength, nature of the salts and the Fe(II)/Fe(III) ratio.

MATERIALS AND METHODS:

Synthesis of Magnetite (Fe_3O_4) Nanoparticles:

0.32 M NaOH solutions were prepared in 200 ml distilled water. A mixture of 0.01M $FeCl_2$ and 0.02M $FeCl_3$ was prepared in 100 ml distilled water. NaOH solution was added slowly to iron salt solution until the pH reached ~8.7. Precipitates, thus obtained, were washed with distilled water and ethanol. The solution was heated to ~100° C to prepare dry powder. Ethanol was added to disperse the magnetite nanoparticles.

Coating of Magnetic Nanoparticles by Aminosilane:

25 ml of above prepared magnetic colloidal ethanol solution was diluted in 150 ml ethanol. The solution was ultrasonicated for 30 minutes. 10 ml 3-aminopropyl -trimethoxysilane (APTES) was added to sonicated product and stirred for 7 hours. The resultant solution was washed five times with methanol after magnetic separation. APTES coated magnetic nanoparticles were dispersed in methanol with 5% concentration.

Surface Modification with PAMAM Dendrimer:

50 ml of freshly prepared Magnetite (Fe_3O_4) Nanoparticle solution was mixed with 200 ml of 20% (V/V) methyl acrylate methanol solution and sonicated at room temperature for 6.5 hrs. particles were then collected via a magnet and rinsed with methanol six times. 40 ml of 50% (V/V) ethylene diamine methanol solution was added to the particles and the suspension was again sonicated for 3 hours. Magnetic separation was then again used to collect particles. Number of generations (G1-G5) were prepared by stepwise growing these nanoparticles using ethylendiamine and methyl acrylate. The resultant product was washed three times with water after magnetic separation.

Antibacterial Study:

The antibacterial activity of magnetite nanoparticles was studied on *Staphylococcus aureus* and *Escherichia coli* strains using well diffusion method as described by Moin *et.al.*[25] The antibacterial activity was identified by the formation of zone of inhibition. The area of the zone of inhibition is the measure of the antibacterial potency of the drug. Larger the zone of inhibition more effective the drug is.

For each bacterium, overnight serial dilutions were made on Mueller Hinton agar (Himedia) to isolate single colonies after 18 hours of incubation at 37° C. Single colonies of bacterium were picked up by a sterilized inoculating loop and subsequently incubated in 25 ml Mueller Hinton broth (Himedia) to obtain pure culture. Individual spread plates for each strain was prepared via sampling 100 µl of this overnight pure culture. 5 wells per plate were cut in the agar plates using disposable graduated 1 ml pipette tip. 20µl, 40µl, 60µl, and 80µl of magnetite NPs sample was loaded in the labeled wells in both the Petri plates. The middle well of the Petri plate was loaded with Streptomycin (50µg/mL positive control antibiotic). Plates were then incubated at 37°C for 20 hours.

RESULTS AND DISCUSSION

The crystalline phase of the prepared nanoparticles was identified by XRD using XPERT-PRO diffract meter (PANalytical –MNIT) equipped with CuKα radiation (λ=0.15406 nm). The optical absorbance of the sample was recorded at room temperature in the wavelength range 200-800 nm using a HR-4000 Ocean Optics (USIC) spectrophotometer. Fourier Transform Infrared Spectroscopy (FTIR) spectra was performed to the dried sample of magnetite using a FTIR – Shimadzu (USIC) spectrophotometer in wave range of 3500 - 4000 cm^{-1} with a resolution of 4 cm^{-1}. Morphological study of NPs and coated NPs were carried out by SEM Carl Zeiss EVO 18 (30 kV) at (USIC-UOR).

X-Ray Diffraction (XRD) of Magnetite NPs:

The XRD results indicate typical X-ray powder diffraction patterns of magnetite nanoparticles (Figure 1). The experimental results were compared with standard magnetite patterns. The XRD patterns show characteristic peaks at 2θ = 30.22º, 35.56º, 43.21º, 53.33º, 57.37º, 62.86º, and 74.55º, marked by (220), (311), (400), (422), (511), (440) with lattice spacing d and lattice parameters a_0.

Figure 1: XRD patterns of Fe_3O_4 Ferrite NPs.

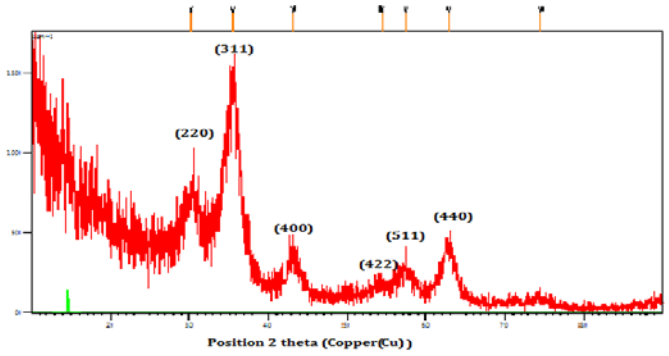

The graph obtained shows that the resultant particles of Fe3O4 are of spinal structure. It is found that the position and relative intensity of the peaks in the obtained XRD patterns match well with the standard magnetite samples according to JCPDS Card No. (79 - 0417). Considering the peak in degrees, particle size has

been estimated by the Scherrer formula. The shape factor has a typical value of about 0.9, but varies with the actual shape of the crystallite; β is the line broadening at full width half maximum. Dhkl is grain size of Magnetite nanoparticle. The particle size was determined by taking the average of sizes at the peaks D220, D311, D400, D422, D511 and D440 and was ~ 18 nm.

Ultraviolet Visible Spectroscopy Analyses of Magnetite NPs:

Figure 2 shows the optical absorption of Fe_3O_4 NPs which is measured in the wavelength range from 200 to 800 nm, with scan interval of 0.2 nm.

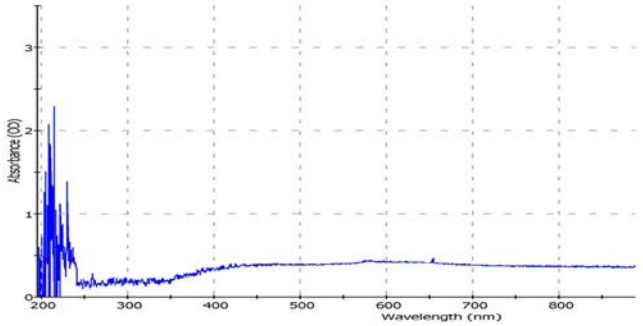

Figure 2: Absorbance A versus wavelength λ (nm) of Fe_3O_4 NPs.

Davis and Mott gave an expression for the absorption coefficient, α(ν), as a function of photon energy (hν) for indirect and direct transition.[20] By plotting $(h\nu\alpha)^{1/2}$ as a function of photon energy (hν), the optical energy band gap for Eg transition can be determined. The respective values of Eg are obtained by extrapolating to $(h\nu\alpha)^{1/2} = 0$ for direct transition as shown in Figure 3.

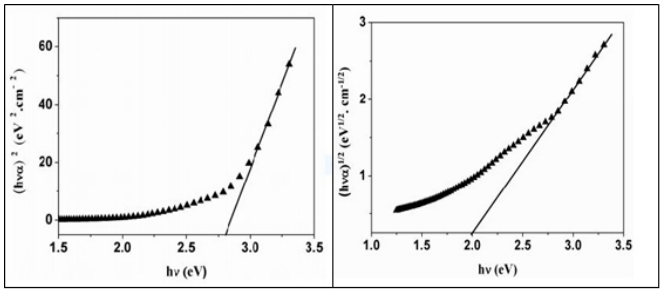

Figure 3: Optical indirect and direct band gap determination of Magnetite using Taucplots.

The values of indirect and direct band gaps of Magnetite are less than as informed by El-Diasty et al. which is due to difference in size (Magnetite in reference has size around 5nm but in the present work it is 18 nm), which means that the energy band gap of the nano materials are inverse proportional to their sizes.[21] The value of direct energy band gap is 2eV and indirect energy band gap is 2.6eV. So sample has been classified as a semiconductor {semiconductor energy band gap (0 - 3 eV)}[22]

Fourier Transform Infrared Spectroscopy Analysis of Magnetite NPs:

Figure 4 demonstrates the FT-IR spectrum of Fe_3O_4 nanoparticles. In pure sample spectrum, presence of absorption bands at 425, 550 and 624 cm^{-1} is associated with Fe-O stretching vibrations of Fe^{2+} and Fe^{3+} ions in octahedral sites and those of Fe^{3+} ions in tetrahedral sites confirm Fe_3O_4 structure formation[23]. FT-IR spectrum shows less intense H-O-H bending vibration in the region 1600 - 1000 cm^{-1}, typical of the H_2O molecule. The second absorption band is between 1000-900 cm^{-1} which corresponds to bending vibration associated to the O – H bond. The O–H bonds in plane and out of plane appears at 1583.45 – 1481.23 and 935.41 – 838.98 cm^{-1}, respectively.[24] These first two bands correspond to the hydroxyl groups attached to hydrogen bonds at the iron oxide surface, as well as the water molecules chemically adsorbed to the magnetic particle surfaces.

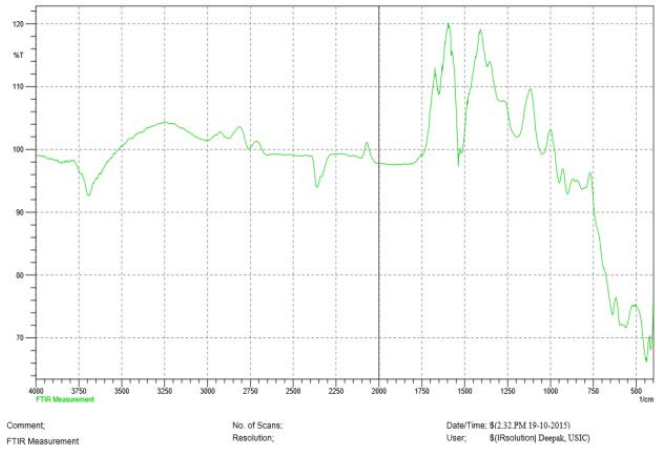

Figure 4: Infrared spectra of the magnetite NPs.

They are characteristically pronounced for all spinal structures for ferrites. In these regions, this occurs because the contributions from the stretching vibration bands related to metal in the octahedral and tetrahedral sites. Thus magnetite nanoparticles have crystalline structure of inverse spinal type and FTIR absorption spectroscopy allowed identifying characteristic features of the spinal structure, as well as a presence of certain types of chemical substances adsorbed on the surface of nanoparticles.

SEM Images of Magnetite NPs:

Figure 5, Figure 6, Figure 7 and Figure 8 illustrate the SEM

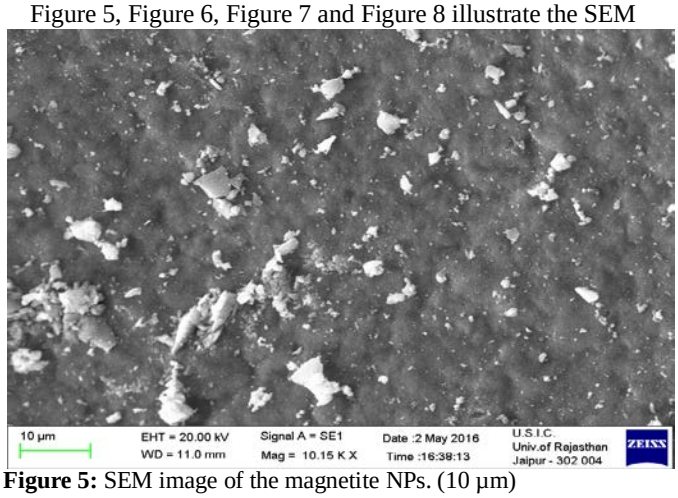

Figure 5: SEM image of the magnetite NPs. (10 µm)

micrograph of the nanoscales magnetite particles. Morphology of the particles was uniform and each particle was approximately ranging between 20 to 70 nm in diameter.

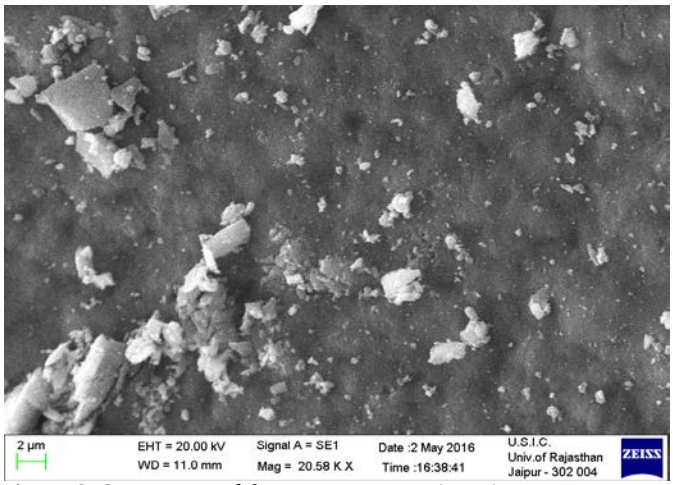

Figure 6: SEM image of the magnetite NPs. (2 µm)

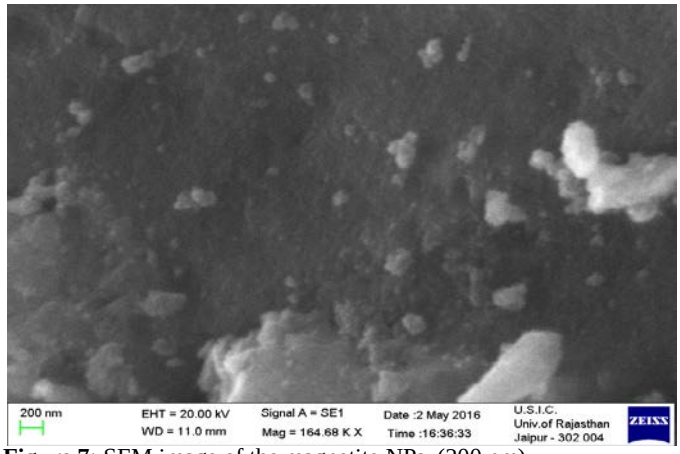

Figure 7: SEM image of the magnetite NPs. (200 nm)

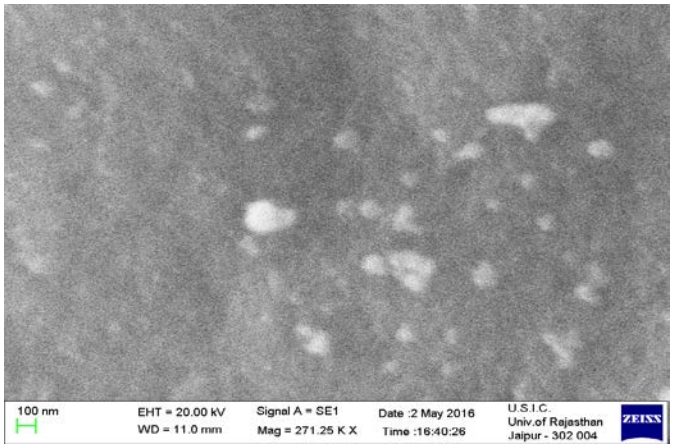

Figure 8:SEM image of the magnetite NPs. (100 nm)

SEM Images of Dendrimer Modified Magnetite NPs:

Figure 9, Figure 10 and Figure 11 illustrate the SEM micrograph at different resolutions of the dendrimer modified magnetite particles. They depict the morphology and size distribution of magnetite nanoparticles modified with APTES and their further number of dendrimer generation.

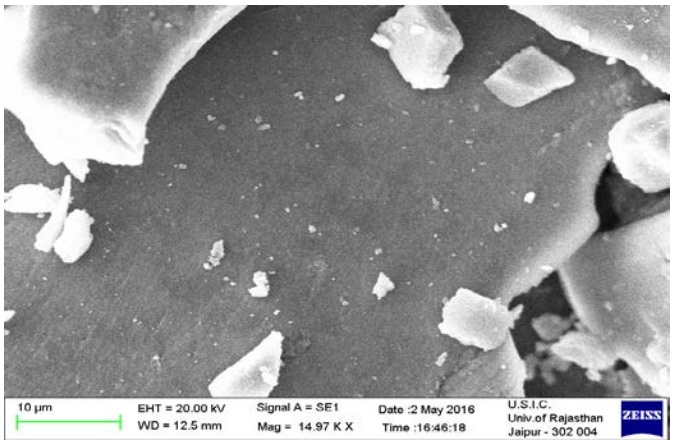

Figure 9: SEM image of the dendrimer modified magnetite NPs. (10 µm)

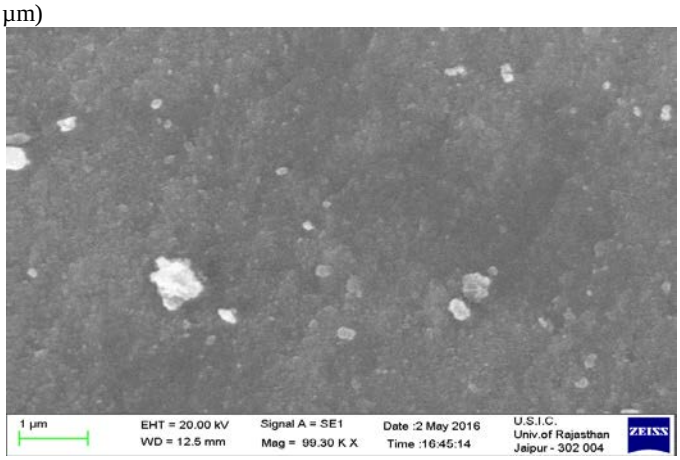

Figure 10: SEM image of the dendrimer modified magnetite NPs. (1 µm)

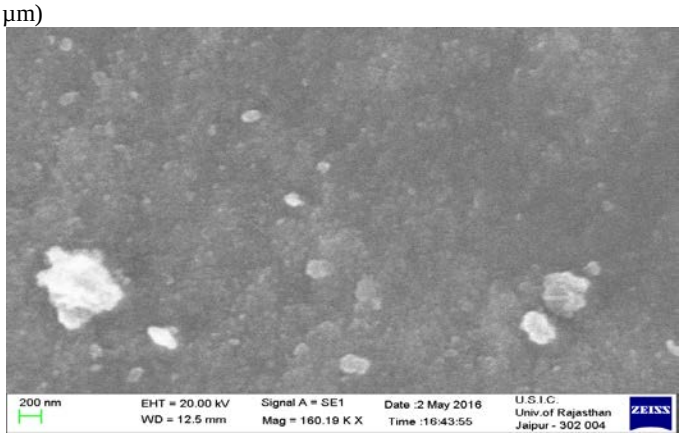

Figure 11: SEM image of the dendrimer modified magnetite NPs. (200 nm)

Antimicrobial Activity analysis

After time interval of 24 hours no antibacterial zone was found around wells containing NPs (Figure 12a and Figure 12b). Circular zone was observed around the antibiotic well which means that these Magnetite particles have shown no activity whereas the activity of the antibiotic was as expected.

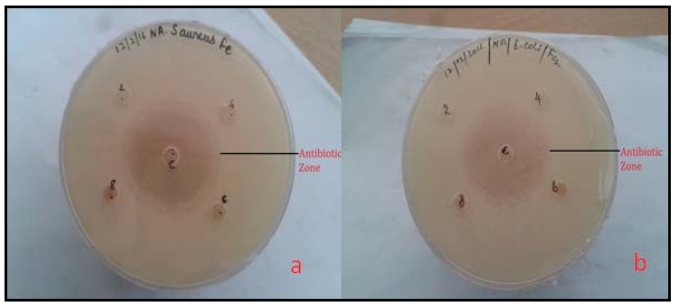

Figure 12: Antimicrobial activity against*Staphylococcus aureus* (Gram-Positive) (12a) and *Escherichia coli* (Gram-negetive) (12b).

CONCLUSION AND FUTURE PROSPECTS:

In this study, superparamagnetic Fe_3O_4 nanoparticles by co-precipitation method and APTEScoated Fe_3O_4 nanoparticles were synthesised. Different physical characteristics of the Fe_3O_4 nanoparticles were studied using IR, UV–Vis, XRD and SEM images. We determined thatthe diameter of Magnetite nanoparticles to be around 18 nm. Optical band gap of Fe_3O_4 nanoparticles was calculated, direct band gap was found to be 2eV and indirect band gap was 2.6eV. No antimicrobial activity was observed as magnetite nanoparticles exhibited no inhibitory activity against both gram-positive bacteria *staphylococcus auries* and gram-negative bacteria *Escherichia coli*.

For the future treatment of cancer, the use of hyperthermia or magnetic material for drug targeting or combining these techniques with surgery, radiotherapy, or chemotherapy will certainly be the subject of intense research. Similarly, synthesis of magnetic material will focus strongly on biocompatible coatings having affinities to different living cells. With the rapid progress of computer technology; fast, powerful and non-expensive results obtained will be used in conjunction with more realistic models for numerical simulation.

REFERENCES

1. S. Bucak, B. Yavuzturk, A. Demir. Magnetic Nanoparticles: Synthesis, Surface Modifications and Application in Drug Delivery. In *Recent Advances in Novel Drug Carrier Systems*; InTech, **2012**.
2. R.A. Sperling, W.J. Parak. Surface modification, functionalization and bioconjugation of colloidal inorganic nanoparticles. *Philos. Trans. R. Soc. A Math. Phys. Eng. Sci.* **2010**, 368 (1915), 1333–1383.
3. A. Mittal, K. Thanki, S. Jain, U. Banerjee. Comparative studies of anticancer and antimicrobial potential of bioinspired silver and silver-selenium nanoparticles. *Applied Nanomedicine*, **2016**, 1(1), 1-6.
4. C.S. Weisbecker, M. V. Merritt, G.M. Whitesides. Molecular Self-Assembly of Aliphatic Thiols on Gold Colloids. *Langmuir* **1996**, 12 (16), 3763–3772.
5. S.-Y. Lin, Y.-T. Tsai, C.-C. Chen, C.-M. Lin, C. Chen. Two-Step Functionalization of Neutral and Positively Charged Thiols onto Citrate-Stabilized Au Nanoparticles. *J. Phys. Chem. B* **2004**, 108 (7), 2134–2139.
6. D. V. Leff, L. Brandt, J.R. Heath. Synthesis and Characterization of Hydrophobic, Organically-Soluble Gold Nanocrystals Functionalized with Primary Amines. *Langmuir* **1996**, 12 (20), 4723–4730.
7. D. Jhanwar, J. Sharma. Chemotherapeutic and chemopreventive effect of ZnO nanoparticles on DMBA/croton oil induced mice skin carcinogenesis. *Applied Nanomedicine*, **2016**, 1(1), 7-11.
8. M. Bhute, Y. Mahant, S. Kondawar. Titanium dioxide / poly(vinylidene fluoride) hybrid polymer composite nanofibers as potential separator for lithium ion battery. *J. Mat. NanoSci.*, **2017**, 4(1), 6-12.
9. P. Raj, D. Mishra, S. Sitaraman, R. Tummala. Nanomagnetic Thinfilms for Advanced Inductors and EMI Shields in Smart Systems. *J. Mat. NanoSci.*, **2014**, 1(1), 31-38.
10. U.O. Ha□feli, J.S. Riffle, L. Harris-Shekhawat, et al. Cell Uptake and in Vitro Toxicity of Magnetic Nanoparticles Suitable for Drug Delivery. *Mol. Pharm.* **2009**, 6 (5), 1417–1428.
11. I. Roy, Anuradha. Synthesis and characterization of iron phosphate NPs and applications in magnetically guided drug delivery. *J. Mat. NanoSci.*, **2016**, 3(1), 1-7.
12. K.-J. Lee, J.-H. An, J.-S. Shin, et al. Biostability of γ-Fe2O3 nano particles Evaluated using an in vitro cytotoxicity assays on various tumor cell lines. *Curr. Appl. Phys.* **2011**, 11 (3), 467–471.
13. K. Gitter, S. Odenbach. Quantitative targeting maps based on experimental investigations for a branched tube model in magnetic drug targeting. *J. Magn. Magn. Mater.* **2011**, 323 (23), 3038–3042.
14. M.G. Krukemeyer, V. Krenn, M. Jakobs, W. Wagner. Mitoxantrone-Iron Oxide Biodistribution in Blood, Tumor, Spleen, and Liver—Magnetic Nanoparticles in Cancer Treatment. *J. Surg. Res.* **2012**, 175 (1), 35–43.
15. M. Kiyama. Conditions for the Formation of Fe 3 O 4 by the Air Oxidation of Fe(OH) 2 Suspensions. *Bull. Chem. Soc. Jpn.* **1974**, 47 (7), 1646–1650.
16. S. Miyamoto. The Effect of Alkali on the Oxidation of Ferrous Hydroxide with Air. *Bull. Chem. Soc. Jpn.* **1927**, 2 (2), 40–44.
17. T. Sugimoto, E. Matijević. Formation of uniform spherical magnetite particles by crystallization from ferrous hydroxide gels. *J. Colloid Interface Sci.***1980**, 74 (1), 227–243.
18. R.N. Laurent, Sophie; Forge, Delphine; Port, Marc; Roch, Alain; Robic, Caroline; Vander Elst, Luce; Muller, S. Laurent, D. Forge, et al. “Magnetic Iron Oxide Nanoparticles: Synthesis, Stabilization, Vectorization, Physicochemical Characterizations, and Biological Applications”. *Chem. Rev.* **2008**, 108 (6), 2064–110.
19. E.A. Davis, N.F. Mott. Conduction in non-crystalline systems V. Conductivity, optical absorption and photoconductivity in amorphous semiconductors. *Philos. Mag.* **1970**, 22 (179), 0903–0922.
20. E.A. Davis, N.F. Mott. , Phil. Mag. () . *Phil. Mag.* **1970**, 22, 903.
21. F. El-Diasty, H.M. El-Sayed, F.I. El-Hosiny, M.I.M. Ismail. Complex susceptibility analysis of magneto-fluids: Optical band gap and surface studies on the nanomagnetite-based particles. *Curr. Opin. Solid State Mater. Sci.* **2009**, 13 (1–2), 28–34.
22. A. Jitianu, M. Raileanu, M. Crisan, et al. Fe3O4–SiO2 nanocomposites obtained via alkoxide and colloidal route. *J. Sol-Gel Sci. Technol.* **2006**, 40 (2–3), 317–323.
23. Z.R. Marand, M.H.R. Farimani, N. Shahtahmasebi. Study of magnetic and structural and optical properties of Zn doped Fe3O4 nanoparticles synthesized by co-precipitation method for biomedical application. *Nanomedicine J.* **2014**, 1 (4), 238–247.
24. L. Zhang, R. He, H.-C. Gu. Oleic acid coating on the monodisperse magnetite nanoparticles. *Appl. Surf. Sci.* **2006**, 253 (5), 2611–2617.
25. S. Moin, S.S. Babu, A. Mahalakshmipriya. In vitro callus production and antibacterial activity of BarlerialupulinaLindl. *AsPac J. Mol. Biol. Biotechnol.* **2012**,20 (2),59–64.